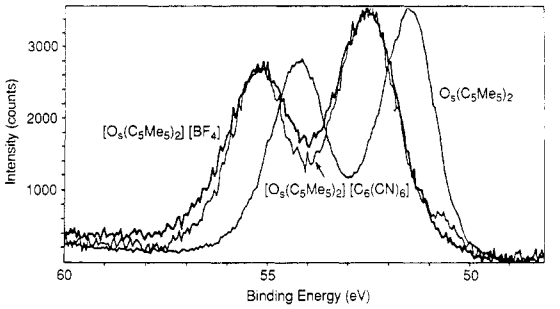

Figure 10. Part of the XPS spectra of $[Os(C_5Me_5)_2]^n$ (n = 0, 1+, 2+) showing the osmium $4f_{7/2}$ and $4f_{5/2}$ photoemission peaks.

Ru Charge-Transfer Salts. The complex $[Ru(C_5Me_5)_2]^{\bullet+}[BF_4]^-$ has been previously reported,[29a] and the EPR indicates that this radical cation shows smaller magnetic anisotropy (Table VIII) than $[M(C_5Me_5)_2]^{\bullet+}$ (M = Fe or Os), even though photoelectron spectroscopy (Table IV) and theoretical considerations conclude that $[Ru(C_5Me_5)_2]^{\bullet+}$ also has an ^2E ground state.[17] Of fundamental interest is the magnetic properties of one-dimensional charge-transfer salts based on this organometallic cation. Unfortunately our experiments have shown that $[Ru^{III}(C_5Me_5)_2]^{\bullet+}$ is very unstable in solution decomposing to the diamagnetic $[Ru^{II}(C_5Me_5)(\eta^6\text{-}C_5Me_4CH_2)]^+$ cation and $Ru^{II}(C_5Me_5)_2$ in ca. 1–2 min in CH_2Cl_2 at −25 °C and almost instantaneously in CH_3CN. The cyclic voltammetry obtained reduction potential of $Ru(C_5Me_5)_2$ is 0.55 V (vs SCE).[29b] Consequently, neither TCNQ nor TCNE is strong enough of an acceptor to oxidize $Ru(C_5Me_5)_2$. Hexacyanobutadiene is strong enough to oxidize $Ru(C_5Me_5)_2$; however, even under rapid precipitation conditions at low-temperature disproportionation dominates and crystalline charge-transfer materials could not be isolated.

X-ray Photoelectron Studies. Core binding energies of a 1, 2, and 3 were measured by XPS to assess the oxidation states of osmium in these materials, and in particular the oxidation state of osmium in compound 3. Figure 10 shows the Os $4f_{7/2}$ and $4f_{5/2}$ photoemission peaks for 1, 2, and 3. A summary of the binding energy values is found in Table X. For 1 the Os $4f_{7/2}$ and $4f_{5/2}$ peaks were found at 51.4 and 54.1 eV. These values fall midway in the range of energies found for the measured Os(II) complexes.[40] For both 2 and 3 the $4f_{7/2}$ and $4f_{5/2}$ peaks were located at 52.4 and 55.1 eV, respectively, indicating a similar charge distribution around the Os centers and in the range found for Os(III) compounds, and so we conclude from these experiments we would assign the oxidation state of osmium in 3 as Os(III). This is inconsistent with the diamagnetic properties, and resolution must await the availability of single crystals suitable for single-crystal X-ray analysis.

Acknowledgment. We wish to thank L. Firment (XPS measurements), M. Ward (electrochemistry), and D. Wipf, S. McLean, B. Carver, and W. Bachmann for their technical assistance.

Registry No. 1, 100603-32-5; 2, 113509-52-7; 3, 113509-53-8; $[NBu_4]^+[C_6(CN)_6]^-$, 58608-56-3; $Ru(C_5Me_5)_2$, 84821-53-4.

Supplementary Material Available: Tables of the least-squares planes and anisotropic thermal parameters (2 pages); a listing of calculated and observed structure factors (2 pages). Ordering information is given on any current masthead page.

(40) Lin'to, I. V.; Zaitsev, B. E.; Molodkin, A.; Ivanova, T. M.; Linko, R. V. *Russ. J. Inorg. Chem. (Engl. Transl.)* **1983**, *26*, 857.
(41) Weimmer, D. E.; Ruben, D. J.; Pines, A. *J. Am. Chem. Soc.* **1981**, *103*, 28.
(42) Cooper, G.; D. Phil. Thesis, Oxford, 1987.
(43) Robbins, J. L.; Edelstein, N. M.; Cooper, S. R.; Smart, J. C. *J. Am. Chem. Soc.* **1979**, *101*, 3853.
(44) Switzer, M. E.; Wang, R.; Rettig, M. F.; Maki, A. H. *J. Am. Chem. Soc.* **1974**, *96*, 7669.
(45) Ting-Tung, T.; Kung, W.-J.; Ward, D. L.; McCulloch, B.; Brubaker, C. H. *Organometallics* **1982**, *1*, 1229.
(46) Andrews, M. P.; Mattar, S. M.; Ozin, G. A. *J. Phys. Chem.* **1986**, *90*, 1037.
(47) Cox, P. A.; Grebenik, P.; Perutz, R. N.; Graham, R. G.; Grinter, R. *Chem. Phys. Lett.* **1984**, *108*, 415.
(48) Perutz, R. N.; Graham, R. G.; Grinter, R., unpublished work.
(49) Duggan, D. M.; Hendrickson, D. N. *Inorg. Chem.* **1975**, *14*, 955.

Electronic Structure of Piano-Stool Dimers. 5. Relationships between the π-Acidity and Electrochemistry in a Series of Isoelectronic Compounds of the Type $Cp_2M_2L_4$ (L = CO, NO)[1]

Bruce E. Bursten,*[2] Roger H. Cayton, and Michael G. Gatter

Department of Chemistry, The Ohio State University, Columbus, Ohio 43210

Received October 16, 1987

The electronic structures of a series of isoelectronic piano-stool dimers of the formulation $[CpM(EO)]_2(\mu\text{-}EO)_2$ (M = Cr, Mn, Fe; E = C, N) have been investigated via nonempirical Fenske–Hall molecular orbital calculations. The π-acid effects of CO vs NO on the frontier orbitals within this system were extracted by comparing the calculated electronic structures with the bonding in the corresponding "σ-only" frameworks, $[CpM(H)]_2(\mu\text{-}H)_2$ (M = Cr, Mn, Fe). These results were then used to explain the directly converse electrochemical results of the iron and chromium dimers. The redox chemistry of these dimers appears to be governed by the nature of the frontier orbitals. For the manganese dimer, the possibility of other geometric isomers has been investigated and predictions have been advanced concerning its yet uninvestigated electrochemistry.

Transition-metal dimers of the general formula $[CpM]_2L_n$ (Cp = $\eta^5\text{-}C_5H_5$), termed piano-stool dimers, comprise a wide class of organometallic compounds displaying a variety of structure types depending on the

0276-7333/88/2307-1342$01.50/0

number and type of ligands L. The synthetic utility of these compounds has been extensively studied, and this bimetallic Cp–M–M–Cp framework has been shown to be an effective template for the coordination and experimental manipulation of a variety of organic substrates.[3] In contrast to the plethora of investigations dealing with the synthesis and reactivity of piano-stool dimers, little is known concerning their electronic structure and bonding. In previous contributions constituting this series we have utilized approximate molecular orbital calculations in order to decipher the electronic effects responsible for some of the anomalous chemical behavior exhibited by dimers in this class.[1,4-6] Not unexpectedly, the electronic structures resulting from such calculations display interesting variations dependent upon the nature of the transition metal, the number and type of ligand L, and the geometry of the complex. Mixed-ligand and heterobimetallic systems further complicate the electronic framework. We have found the calculations to be particularly useful when applied to those systems that contain bridging ligands, inasmuch as ligand bridges can greatly complicate the simple bonding schemes derived from joining two monomeric units.

In this contribution, we will focus on the piano-stool dimer system *trans*-$[CpM(EO)]_2(\mu\text{-}EO)_2$, where M = Cr, E = N,[7,8] or M = Fe, E = C,[9] or M = Mn, E = C, N.[8] Fenske–Hall MO calculations have been performed on this isoelectronic series in order to discern the effects of varying the π-acid ligand (CO, NO) on the orbital energetics and bonding. It will also be shown that the resulting descriptions of the electronic structures offer a rational explanation of the observed electrochemistry within this series.

The π-acid strength of CO vs NO coordinated to transition metals has recently been the subject of several theoretical investigations involving the related piano-stool dimer system $[CpM(\mu\text{-}EO)]_2$ (M = Fe, Co, Ni; E = C, N.)[10-12] These studies have shown that the substitution of a μ-CO ligand with a μ-NO ligand leads to a significant perturbation in the frontier orbital energetics, resulting in variations in their relative stabilities as well as reactivities. The chemistry of the $[CpML]_2(\mu\text{-}L)_2$ system appears to be equally diverse and as dependent on the electronic effects induced by the bonding of the π-acid ligands CO and NO.

In order to best reveal the relative electronic effects of altering the π-acid ligands, we will first construct the geometrically appropriate piano-stool dimer framework

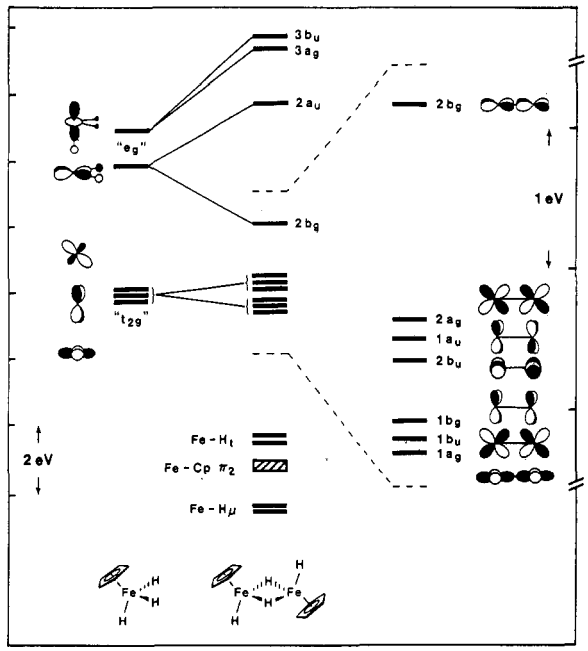

Figure 1. Molecular orbital diagram for the frontier region of $[CpFeH]_2(\mu\text{-}H)_2$. The right side displays the metal-based orbitals $1a_g$–$2b_g$.

consisting exclusively of "σ-only" ancillary ligands, i.e. $[CpM(H)]_2(\mu\text{-}H)_2$ (M = Cr, Mn, Fe). The hydride ligands will then be replaced by π-acid ligands, and the effects on the relevant dimer orbitals will be traced so as to determine the π influences associated with these ligands. This approach will prove particularly useful in determining the derivation and fate of the dimer orbitals in terms of simpler transition-metal fragments. The details of the calculations are provided in the Appendix.

$[CpM(H)]_2(\mu\text{-}H)_2$: σ-Only Framework

The structure of each of the *trans*-$[CpM(EO)]_2(\mu\text{-}EO)_2$ dimers is shown in I. If each Cp ring is assumed to occupy

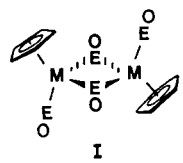

I

three coordination sites, the structure is formally that of an edge-sharing bioctahedron. We will see later that this analogy is borne out electronically as well as structurally. The MO diagram of the fictitious "σ-only" species $[CpM(H)]_2(\mu\text{-}H)_2$ is shown in Figure 1 for M = Fe (analogous results are obtained for M = Cr or Mn).[13] Since the hydride ligands can only interact with the transition-metal orbitals in a σ fashion, they will be used to model the σ interactions of the CO or NO ligands. Of course, the σ-donor strength of the hydride ligand will differ from that of the CO or NO ligand; however, the same metal-based orbitals will be involved in either case, and the overall magnitude of these interactions will not be important. Moreover, the orbitals resulting from M–L σ interactions will not lie in the crucial frontier region. What is important is that the hydride ligands will leave the metal–ligand π-type orbitals unperturbed such that subsequent re-

(1) For part 4 of this series see: Bursten, B. E.; Cayton, R. H. *J. Am. Chem. Soc.* **1987**, *109*, 6053–6059.
(2) Camille and Henry Dreyfus Foundation Teacher-Scholar (1984–1989) and Fellow of the Alfred P. Sloan Foundation (1985–1987).
(3) See, for example: *Comprehensive Organometallic Chemistry*; Wilkinson, G., Stone, F. G. A., Abel, E. W., Eds.; Pergamon: Oxford, 1982; Vols. 3–6.
(4) Blaha, J. P.; Bursten, B. E.; Dewan, J. C.; Frankel, R. B.; Randolph, C. L.; Wilson, B. A.; Wrighton, M. S. *J. Am. Chem. Soc.* **1985**, *107*, 4561–4562.
(5) Bursten, B. E.; Cayton, R. H. *Organometallics* **1986**, *5*, 1051–1053.
(6) Bursten, B. E.; Cayton, R. H. *J. Am. Chem. Soc.* **1986**, *108*, 8241–8249.
(7) (a) Kolthammer, B. W. S.; Legzdins, P. *J. Chem. Soc., Dalton Trans.* **1978**, 31–35. (b) Kolthammer, B. W. S.; Legzdins, P.; Malito, J. T. *Inorg. Synth.* **1979**, *19*, 208–212.
(8) (a) King, R. B.; Bisnette, M. B. *J. Am. Chem. Soc.* **1963**, *85*, 2527. (b) King, R. B.; Bisnette, M. B. *Inorg. Chem.* **1964**, *3*, 791–796.
(9) (a) Piper, T. S.; Cotton, F. A.; Wilkinson, G. *J. Inorg. Nucl. Chem.* **1955**, *1*, 165. (b) King, R. B.; Stone, F. G. A. *Inorg. Synth.* **1963**, *7*, 110–112.
(10) Pinhas, A. R.; Hoffmann, R. *Inorg. Chem.* **1979**, *18*, 654–658.
(11) (a) Schugart, K. A.; Fenske, R. F. *J. Am. Chem. Soc.* **1986**, *108*, 5094–5100. (b) Schugart, K. A.; Fenske, R. F. *J. Am. Chem. Soc.* **1986**, *108*, 5100–5104.
(12) Demuynck, J.; Mougenot, P.; Benard, M. *J. Am. Chem. Soc.* **1987**, *109*, 2265–2267.

(13) Strictly speaking, $[CpFeH]_2(\mu\text{-}H)_2^{4-}$ would be isoelectronic to 1; however, we are primarily interested in the nature and energetics of the orbitals of the σ-only framework; hence we have made no attempt to indicate orbital occupany in the fictitious hydride frameworks.

placement with a π-acid ligand will produce a clear picture of the π-back-bonding interactions. The metal-based orbitals of $[CpFe(H)]_2(\mu\text{-}H)_2$ can be conveniently separated into two groups: the "pseudo-t_{2g}" set comprised of the lower lying set of six orbitals ($1a_g$, $1b_u$, $1b_g$, $2b_u$, $1a_u$, $2a_g$) and the "pseudo-e_g" set consisting of four orbitals ($2b_g$, $3b_u$, $3a_g$, $2a_u$). The basis for referring to these groups as pseudo-t_{2g} and pseudo-e_g is built upon the structural analogy of this framework to the bioctahedron, wherein the metals are in pseudo-O_h symmetry. In the spirit of Hoffmann's isolobal analogy,[14] each metal center "remembers" its octahedral electronic parentage; hence its metal-based d orbitals are split (as if by an O_h field) into two distinct groups resembling the O_h t_{2g} and e_g sets.[15] The four orbitals of the "e_g" set have their lobes pointed directly at the hydride ligands, three of which ($2a_u$, $3a_g$, $3b_u$) are M–H σ^* in character and are consequently destabilized with respect to the $2b_g$ orbital which is of incorrect symmetry to interact with the H ligands and hence is only destabilized by its interaction with the Cp ligands. It is easy to see the derivation of these four orbitals from the pseudo-e_g set of a three-legged piano-stool monomer. They are simply the symmetric and antisymmetric combinations of the orbitals of two such fragments. Likewise, the "t_{2g}" set consists of six metal-based orbitals which are the symmetric and antisymmetric combinations of the three pseudo-t_{2g} orbitals of two monomeric three-legged piano-stool fragments. Since the orbitals of the "t_{2g}" set have no hydride and little Cp character, they are split only through M–M interaction into three lower lying bonding orbitals and three M–M antibonding orbitals at slightly higher energy. However, even at an Fe–Fe distance of 2.534 Å (that found in *trans*-$[CpFe(CO)]_2(\mu\text{-}CO)_2$[16] there is no appreciable direct metal–metal bonding as evidenced by the minimal splitting within the "t_{2g}" set (<1.0 eV). The absence of a strong Fe–Fe interaction appears to be the result of hybridization induced by the μ-L σ-bonding interactions. The symmetric Fe d_{z^2} combination (z axis along Fe-Fe vector), which would form an Fe–Fe σ bond, mixes with a symmetric combination of Fe $d_{x^2-y^2}$ orbitals to produce two new metal-based hybrid orbitals as shown.

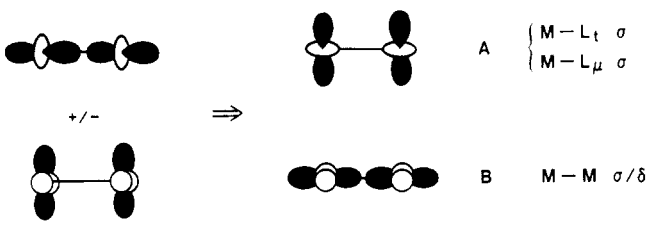

One of these hybrids (A) interacts with the symmetric combination of μ-L σ orbitals, while the other hybrid orbital (B) remains as an essentially nonbonding metal-based orbital that is ca. 50% σ and ca. 50% δ in character. From here on, this metal-based hybrid will be referred to as the M–M σ/δ bonding orbital. The result is the removal of a strong, direct Fe–Fe bond (pure d_{z^2} interaction) due to μ-L σ interaction that, upon hybridization, yields a much weaker Fe–Fe bonding interaction (σ/δ hybrid B). A similar hybridization is found to occur in the $2b_u$ orbital. Direct dimerization of the $CpFeH_3$ "t_{2g}" orbitals would produce a b_u orbital similar in shape to the $1a_g$ orbital, but Fe–Fe antibonding in character. However, an allowed mixing takes place with a higher energy b_u orbital ($3b_u$)

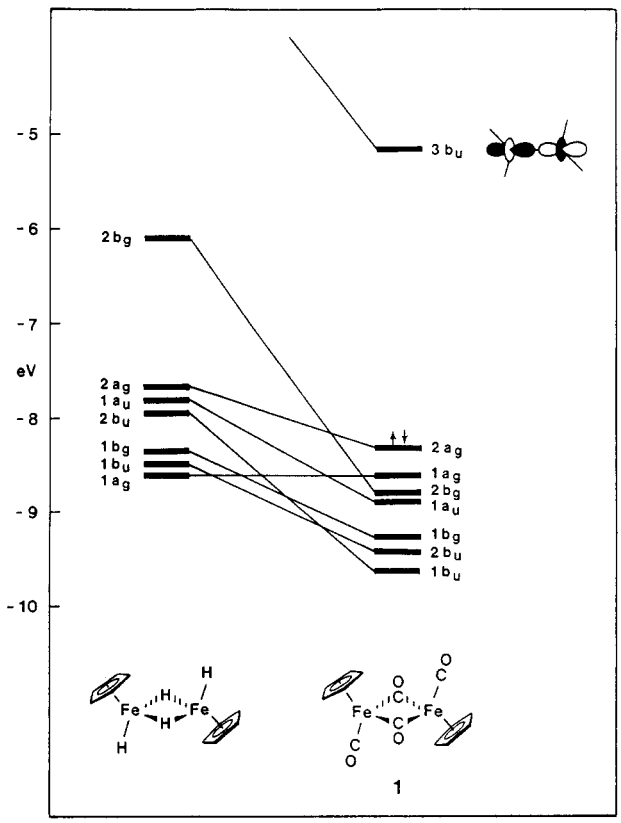

Figure 2. Molecular orbital diagram displaying the frontier orbital region of $[CpFe(CO)]_2(\mu\text{-}CO)_2$ (1) (right side) and its correlation to the orbitals of $[CpFeH]_2(\mu\text{-}H)_2$ (left side). The arrows indicate the highest occupied MO.

to cause a rehybridization and produce the observed $2b_u$ orbital as shown.

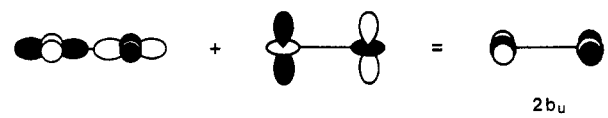

This mixing serves to weaken the Fe–Fe antibonding character of the $2b_u$ orbital.

The far right side of Figure 1 expands a section of the MO diagram such that orbitals $1a_g$–$2b_g$ may be shown pictorially. These are the metal-based orbitals that are of the correct symmetry to interact in a π fashion with the ancillary ligands. We will examine these interactions in the next section as the hydride ligands will be replaced by CO ligands.

$[CpFe(CO)]_2(\mu\text{-}CO)_2$

Replacement of the four hydride ligands with four carbonyl ligands affords the well-known species $[CpFe(CO)]_2(\mu\text{-}CO)_2$ (1). Figure 2 depicts the frontier MO diagram for this compound along with the correlation of its orbitals to those of the tetrahydrido dimer. Only the metal-based orbitals derived from the expanded section of Figure 1 are shown here since only these orbitals are further affected by the formal replacement of the σ-only hydride ligands with the π-acid CO. The remainder of the orbital picture is essentially the same as that in Figure 1 for $[CpFe(H)]_2(\mu\text{-}H)_2$.[17] Although the Fenske–Hall method,[6] as well as several other MO formalisms of varying rigor,[18-21] has been applied to this dimer, some new ob-

(14) Hoffmann, R. *Science (Washington, DC)* **1981**, *211*, 995–1002.
(15) The splitting into pseudo-t_{2g} and pseudo-e_g sets refers to a ligand field effect exclusively.
(16) Mitschler, A.; Rees, B.; Lehmann, M. S. *J. Am. Chem. Soc.* **1978**, *100*, 3390–3397.
(17) The Fe–CO σ interactions are located at slightly different energies than the corresponding Fe–H orbitals. See ref 6 for details of these Fe–CO σ interactions.

Table I. Percent Characters of the Highest Occupied and Lowest Unoccupied Orbitals of Compounds 1, 2, and 3

1				2				3			
orbital	type[a]	% Fe	% CO[b]	orbital	type[a]	% Cr	% NO[b]	orbital	type[a]	% Mn	% CO/NO[b]
				$4b_u$	σ^*	82	10	$4b_u$	π	38	0/55
				$3b_g$	δ	11	83	$3b_g$	π^*	27	1/62
$3b_u$	σ^*	79	11	$3b_u$	π	16	75	$3b_u$	σ^*	81	5/9
$2a_g$[c]	π^*	89	8	$2a_g$[c]	σ/δ	96	0	$2a_g$[c]	π^*	78	11/6
$1a_g$	σ/δ	96	0	$1a_g$	π^*	57	38	$1a_g$	σ/δ	91	5/1
$2b_g$	π^*	54	36	$1a_u$	δ^*	55	41	$1a_u$	δ^*	70	18/8
$1a_u$	δ^*	81	15	$2b_g$	π^*	54	41	$2b_g$	π^*	63	27/2
$1b_g$	δ	79	17	$2b_u$	π	48	47	$1b_g$	δ	58	7/29
$2b_u$	π	76	22	$1b_u$	σ^*/δ^*	41	51	$2b_u$	π	57	1/37
$1b_u$	σ^*/δ^*	65	27	$1b_g$	δ	33	59	$1b_u$	σ^*/δ^*	41	1/50

[a] Refers to type of M–M interaction. [b] 2π character only. [c] HOMO.

servations can be extracted from the type of analysis advanced here.

(1) The $1a_g$ orbital, which is the σ/δ hybridized Fe–Fe bonding orbital, is not able to interact with the 2π orbitals of either terminal or bridging CO ligands and therefore is unperturbed by the replacement of H with CO. This orbital becomes the SHOMO (second highest occupied MO) of 1. (2) One orbital of the "e_g" set, the $2b_g$, can interact with the μ-CO 2π orbitals and does so substantially such that it becomes stabilized among the orbitals of the "t_{2g}" set. (3) The remaining five "t_{2g}"-based orbitals all interact with either bridging and/or terminal CO 2π orbitals and are all stabilized to a similar degree. (4) The $2a_g$ orbital is stabilized only by t-CO 2π (t = terminal) interaction, and it is the only "t_{2g}"-based orbital that remains above the Fe–Fe σ/δ ($1a_g$) orbital. Consequently the $2a_g$ orbital, which is primarily Fe–Fe π^* in character, becomes the HOMO of the tetracarbonyl dimer, a factor which will prove to be important during the interpretation of its electrochemical data.

$[CpCr(NO)]_2(\mu\text{-}NO)_2$

We are now in position to replace the four hydride ligands with NO ligands and examine their effects on the dimer electronic structure in light of those discussed above for CO. We will accomplish this by considering the dimer $[CpCr(NO)]_2(\mu\text{-}NO)_2$ (2), which is isoelectronic with 1. The comparative bonding capabilities of CO and NO have been the subject of numerous prior investigations.[22] The most significant electronic difference resides in the energy of the respective 2π orbitals (π-back-bonding orbitals). The 2π orbitals of NO are substantially lower in energy than are the CO 2π orbitals, thereby allowing a better energy match between the NO 2π and metal-based orbitals and thus providing a stronger interaction. Calculations performed on these dimers, and those presented in the following paper, indicate that the NO 2π orbitals interact approximately twice as strongly as CO 2π orbitals with similar metal-based d orbitals, as based on the percent NO 2π orbital contributions to the MO's of the dimer (see Table I). This stronger interaction found for the NO ligands is

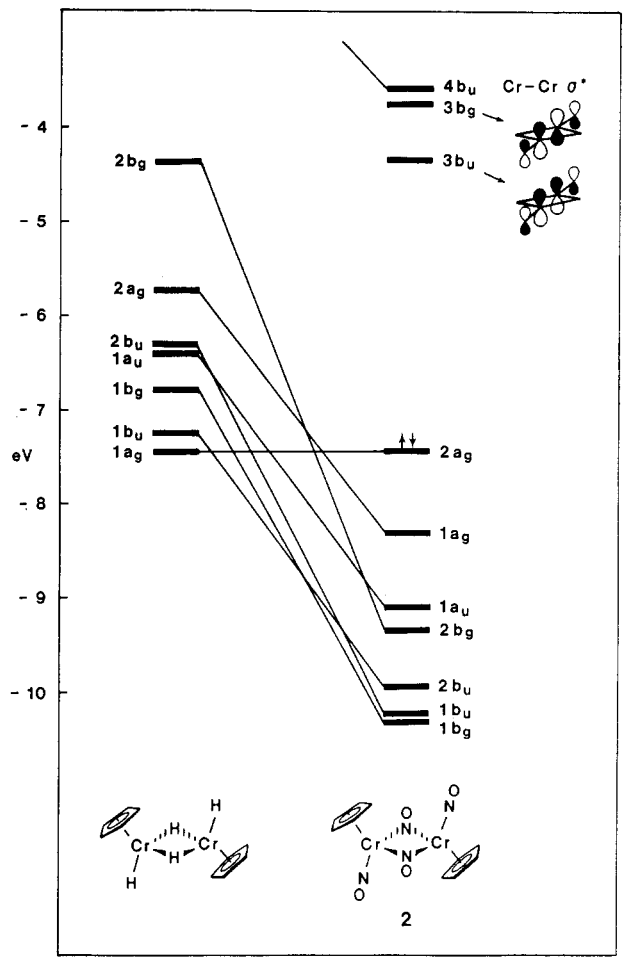

Figure 3. Molecular orbital diagram displaying the frontier orbital region of $[CpCr(NO)]_2(\mu\text{-}NO)_2$ (2) (right side) and its correlation to the orbitals of $[CpCrH]_2(\mu\text{-}H)_2$ (left side). The arrows indicate the highest occupied MO.

clearly evident in the MO diagram of 2 shown in Figure 3. As before, only the metal-based orbitals and their correlation to the metal-based orbitals of the corresponding chromium tetrahydrido dimer are shown. It is worthwhile to note that, in going from $[CpFe(H)]_2(\mu\text{-}H)_2$ to $[CpCr(H)]_2(\mu\text{-}H)_2$, neither the character nor the relative energetics of the metal-based orbitals is significantly altered, although the orbitals of the Cr framework are shifted in a nearly uniform fashion to higher energy (ca. 1.5 eV). A comparison of the MO diagram in Figure 3 to that of 1 (Figure 2) allows us to highlight several interesting features. First, the Cr-based orbitals show a greater degree of stabilization when compared to those of the Fe dimer, direct evidence of the stronger NO 2π interaction with the Cr d orbitals compared to the CO 2π interaction with the corresponding Fe d orbitals. Although the reason for this was

(18) Granozzi, G.; Tondello, E.; Benard, M.; Fragalá, I. *J. Organomet. Chem.* **1980**, *194*, 83–89.
(19) Jemmis, E. D.; Pinhas, A. R.; Hoffmann, R. *J. Am. Chem. Soc.* **1980**, *102*, 2576–2585.
(20) Benard, M. *J. Am. Chem. Soc.* **1978**, *100*, 7740–7742.
(21) Benard, M. *Inorg. Chem.* **1979**, *18*, 2782–2785.
(22) (a) Bursten, B. E.; Jensen, J. R.; Gordon, D. J.; Treichel, P. M.; Fenske, R. F. *J. Am. Chem. Soc.* **1981**, *103*, 5226–5231. (b) Avanzino, S. C.; Bakke, A. A.; Chen, H.-W.; Donahue, C. J.; Jolly, W. L.; Lee, T. H.; Ricco, A. J. *Inorg. Chem.* **1980**, *19*, 1931–1936. (c) Fenske, R. F.; Jensen, J. R. *J. Chem. Phys.* **1979**, *71*, 3374–3382. (d) Chen, H.-W.; Jolly, W. L. *Inorg. Chem.* **1979**, *18*, 2584–2551. (e) Hoffmann, R.; Chen, M. M. L.; Elian, M.; Rossi, A. R.; Mingos, D. M. P. *Inorg. Chem.* **1974**, *13*, 2666–2675. (f) Hillier, I. H.; Guest, M. F.; Higginson, B. R.; Lloyd, D. R. *Mol. Phys.* **1974**, *27*, 215–223. (g) Lloyd, D. R.; Schlag, E. W. *Inorg. Chem.* **1969**, *8*, 2544–2555.

briefly described above, it will be instructive to look at it somewhat more quantitatively here. Inherent to any MO method derivative of the Wolfsberg–Helmholz formalism (such as Fenske–Hall or extended Hückel theory[23]) is the assumption that the degree of interaction between two orbitals is primarily dependent upon two factors: (1) the overlap of the two orbitals and (2) the energy differential between the interacting orbitals. In the case at hand, the energy differential (ΔE) weighs as the more important criterion. The closer the energy match between interacting orbitals (smaller ΔE), the greater the interaction. In **2**, the energetic separation between the Cr 3d and the NO 2π orbitals is only 1.45 eV, whereas the corresponding value in **1** is 6.28 eV. This also induces changes in the HOMO and LUMO of **2** relative to **1**. In the Cr dimer, the HOMO is the $2a_g$ orbital corresponding to the Cr–Cr σ/δ bonding interaction. This contrasts to that found in the Fe dimer, which, albeit also an a_g orbital, was Fe–Fe π^* in character. The LUMO of the Fe dimer (Figure 2) is essentially an Fe–Fe σ^* orbital composed primarily of Fe d_{z^2} character (73%). As is evident, in Figure 3, the corresponding Cr–Cr σ^* orbital ($4b_u$), while unoccupied, is not the LUMO of the Cr dimer. There are two virtual orbitals, $3b_g$ and $3b_u$, which lie at slightly lower energy than the $4b_u$ orbital, and both of these are localized on the μ-NO lignds. They represent the symmetric and antisymmetric combinations of the μ-NO 2π orbitals that are oriented perpendicular to the plane of the dimetallacyclic core. We will see how these variations between the HOMO's and LUMO's of the Fe and Cr dimers affect the electrochemistry of these species in the next section.

One final point of note before we move to the discussion of the electrochemistry concerns the formal designations of terminal NO ligands as NO^+ and bridging NO ligands as NO^-. Looking at the metal-based orbitals in Figure 3 and focussing on the two lowest ($1b_g$ and $1b_u$), we see that they are composed of greater NO character than Cr character (see Table I). Therefore these two orbitals are more *ligand-based* rather than *metal-based*, and the ligand character is primarily from the bridging nitrosyls. This supports the notion that bridging NO ligands have a greater degree of occupation of their 2π orbitals than do the terminal NO ligands and could be considered NO^- in the limiting case.

Electrochemistry of $[CpFe(CO)]_2(\mu\text{-}CO)_2$ and $[CpCr(NO)]_2(\mu\text{-}NO)_2$

Electrochemistry, and in particular cyclic voltammetry, provides a valuable probe into the frontier orbitals of molecules.[24] The electrochemistry of both **1**[25] and **2**[26] has been investigated and exhibits very interesting results, especially in light of the theoretical descriptions discussed earlier. These results can be conveniently summarized in eq 1 and 2.

The iron dimer (eq 1) undergoes an irreversible two electron reduction to yield two monomeric anions. This reaction can also be accomplished chemically, of course, with a suitable reducing agent, e.g. Na/Hg.[27] One electron oxidation was found to be reversible, producing a bimetallic radical cation. Just the opposite results were found for the isoelectronic chromium dimer (eq 2). **2** is cleaved into

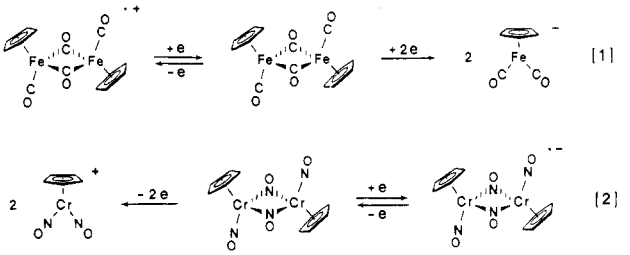

two monomeric cations upon an irreversible two-electron oxidation, whereas reduction is a reversible, one-electron process yielding the isolable bimetallic radical anion.

These seemingly anomalous results can be readily understood with the aid of the MO diagrams of each of the parent dimers. We will begin with the iron carbonyl dimer (Figure 2). The HOMO is metal-based and primarily Fe–Fe π^* in character. Oxidation would presumably result in removal of electrons from this orbital and thereby strengthen the weak Fe–Fe interaction. This is consistent with experiment inasmuch as the dimer remains intact upon oxidation. On the other hand, the LUMO of **2** was calculated to be energetically isolated and strongly Fe–Fe σ^* in character. Reduction would result in adding electrons to this orbital, thus weakening the Fe–Fe interaction. This also appears to be consistent with experiment in that the reduction of the complex causes the irreversible cleavage of the dimer into two stable monomeric two-legged piano-stool anions.

We can apply a similar analysis to explain the directly opposite results found for the isoelectronic chromium dimer. As was mentioned earlier, the character of both the HOMO and LUMO of **2** differ from those of **1**. The HOMO of the Cr dimer ($2a_g$) is the Cr–Cr σ/δ bonding interaction. Although this orbital represents a relatively weak Cr–Cr interaction, it is the strongest of the "t_{2g}" set. Oxidation, and hence removal of electrons from the Cr–Cr σ/δ bond, should weaken the Cr–Cr interaction. Upon oxidation, neither the dimeric cation ($\mathbf{2}^+$) or dication ($\mathbf{2}^{2+}$) has been observed; rather, cleavage into monomeric products occurs. Two electron oxidation of **2** would yield an electronically unsaturated, formally d^4–d^4 dimer with a severely weakened Cr–Cr bond. Apparently, in the presence of even very weak Lewis bases such as PF_6^- or BF_4^-, the driving force to form monomeric d^6 three-legged piano-stool complexes is great enough to facilitate the cleavage of the dimer. Thus, the oxidation of **2** by HBF_4 in MeCN leads to the formation of $[CpCr(NO)_2(NCMe)]^+[BF_4]^-$.[28] When the same reaction is run in a noncoordinating solvent such as CH_2Cl_2, the product is characterized as $CpCr(NO)_2(FBF_3)$,[28] analogous to $CpCr(NO)_2(FPF_5)$,[29] which was prepared by a different route.

The LUMO of **2** was shown to be composed almost entirely (75%) of μ-NO 2π character. This orbital is the symmetric combination of the μ-NO 2π orbitals oriented perpendicular to the bridge plane such that their interaction with the metal-based orbitals is minimal. The dimer was shown to undergo reversible one-electron reduction, and a bimetallic radical anion could be isolated. The ESR spectrum of this radical anion indicates strong coupling of the electron to one type of nitrogen atom ($a_{N_1} = 5.89$ G) and weaker couplings to a second type of nitrogen atom ($a_{N_2} = 0.89$ G).[26] The IR spectrum of the radical anion displays two strong absorptions at 1580 and 1331 cm^{-1} attributable to terminal and bridging NO stretches re-

(23) Hoffmann, R. *J. Chem. Phys.* **1963**, *39*, 1397–1412.
(24) (a) Bard, A. J.; Faulkner, L. R. *Electrochemical Methods, Fundamentals and Applications*; Wiley: New York, 1980. (b) Bursten, B. E.; Green, M. R. *Prog. Inorg. Chem.*, in press.
(25) Ferguson, J. A.; Meyer, T. J. *Inorg. Chem.* **1971**, *10*, 1025–1028.
(26) Legzdins, P.; Wassink, B. *Organometallics* **1984**, *3*, 1811–1817.
(27) Piper, T. S.; Wilkinson, G. *J. Inorg. Nucl. Chem.* **1956**, *3*, 104.
(28) Legzdins, P.; Martin, D. T.; Nurse, C. R.; Wassink, B. *Organometallics* **1983**, *2*, 1238–1244.
(29) Regina, F. J.; Wojcicki, A. *Inorg. Chem.* **1980**, *19*, 3803–3807.

spectively.[26] These absorptions appear 90 and 175 cm^{-1}, respectively, lower in energy than those exhibited by the neutral parent dimer, thus providing further support for the substantial localization of the extra electron in the radical anion onto the 2π orbitals of the NO ligands, and in particular the μ-NO ligands. These experimental results are all consistent with our calculational finding that the LUMO of the neutral parent dimer is localized primarily on the μ-NO 2π orbitals.

It is of interest to note that both the reductive cleavage of **1** and the oxidative cleavage of **2** are two-electron processes. This seems consistent with the nature of the orbitals involved in the redox processes. In **1**, electrons are being added to the LUMO, an Fe–Fe σ^* orbital. Addition of one electron to the LUMO to generate "$[CpFe(CO)_2]_2^-$" ($\mathbf{1}^-$) would presumably be accompanied by an increase in the Fe–Fe distance relative to the neutral dimer. As a result, the σ^* orbital of $\mathbf{1}^-$ will fall in energy relative to that of **1**, ignoring the difference in charge between the two dimers. If one adopts the common view that oxidation and reduction potentials of molecules are related to the HOMO and LUMO energies, respectively,[24] it is seen that $\mathbf{1}^-$ should be reduced at a lower potential than **1**; i.e., $\mathbf{1}^-$ is expected to be unstable with respect to disproportionation into **1** and $CpFe(CO)_2^-$. If the kinetics of electron transfer are fast relative to the cyclic voltammetry, an apparent two-electron process will be seen. Similarly, the oxidation of **2** involves the removal of electrons from a Cr–Cr σ orbital. By analogy, the removal of one electron to form the hypothetical $\mathbf{2}^+$ species would lead to an increase in the Cr–Cr distance, a rise in the energy of the σ orbital, a lower oxidation potential for $\mathbf{2}^+$ than for **2**, and, again if the kinetics are favorable, an apparent two-electron oxidation. This argument, while undoubtedly overly simplistic, is consistent with the observed chemical oxidation of **2**: if the dimer is treated with 1 equiv of HBF_4, only half of the starting material reacts and there is no evidence for the formation of $\mathbf{2}^+$ as an intermediate.[28]

$[Cp_2Mn_2(CO)(NO)](\mu\text{-}CO)(\mu\text{-}NO)$

We have seen the variation in electronic structure associated with replacing the hydride ligands of $[CpM(H)]_2(\mu\text{-}H_2)$ with moderate π-acid ligands (CO) and subsequently with stronger π-acid ligands (NO). In this section we will discuss the electronic effects of a mixed-ligand system involving the ligation of both CO and NO ligands to a single piano-stool dimer framework. The known compound $[Cp_2Mn_2(CO)(NO)](\mu\text{-}CO)(\mu\text{-}NO)$ (**3**) satisfies these criteria and is isoelectronic with the diiron tetracarbonyl and dichromium tetranitrosyl systems discussed above. This compound contains both t-CO and μ-CO ligands as well as t-NO and μ-NO ligands in solution and in the solid state as evidenced by IR spectroscopy.[30] The MO diagram of **3** is presented in Figure 4, along with the correlation of its orbitals to those of $[CpMn(H)]_2(\mu\text{-}H)_2$. Due to the coordination modes of the CO and NO ligands, the symmetry of **3** is reduced from C_{2h} to C_1. However, the C_{2h} symmetry labels have been retained in order to clarify the orbital derivation as well as to aid in their discussion.

The filled Mn-based orbitals are separated into two distinct sets: a lower set of three orbitals ($1b_u$, $2b_u$, $1b_g$) that are involved primarily in Mn–NO π back-bonding and an upper set of four orbitals ($2b_g$, $1a_u$, $1a_g$, $2a_g$), three of which are Mn–CO π back-bonding and one of which ($1a_g$)

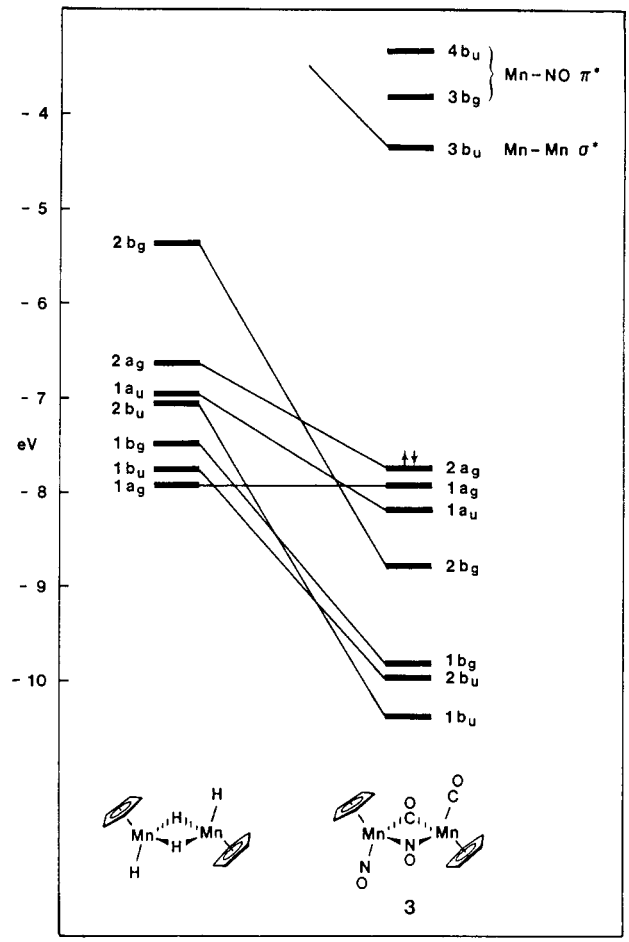

Figure 4. Molecular orbital diagram displaying the frontier orbital region of $[Cp_2Mn_2(CO)(NO)](\mu\text{-}CO)(\mu\text{-}NO)$ (**3**) (right side) and its correlation to the orbitals of $[CpMnH]_2(\mu\text{-}H)_2$ (left side). The arrows indicate the highest occupied MO.

is once again left relatively unperturbed (>90% Mn in character) when the H ligands are replaced with π-acid ligands. The orbital energetics within this upper set of Mn-based orbitals resemble those of **1** (Figure 2) most notably in that the HOMO is Mn–Mn π^* in character and the SHOMO represents the Mn–Mn σ/δ bonding orbital.

Once again, the greater stabilization of the metal-based Mn–NO orbitals compared to the metal-based Mn–CO orbitals can be traced back to the more favorable energy differential between the Mn d orbitals and the NO 2π orbitals (ΔE = 2.28 eV) compared to the Mn d orbitals and the CO 2π orbitals (ΔE = 5.86 eV).[31]

The virtual orbitals of **3** show similarities to the virtual orbitals of both the iron and chromium dimers. The LUMO of **3** is Mn–Mn σ^* (similar to the LUMO of the Fe dimer), and at slightly higher energy are two ligand-based orbitals of primarily NO 2π character (similar to the LUMOs of the Cr dimer).

To our knowledge, the electrochemistry of **3** has not been reported. On the basis of the calculated electronic structure, however, we are able to conjecture on the results of its oxidation or reduction. The HOMO of **3** is Mn–Mn π^* in character and similar to that of the iron dimer, which undergoes reversible oxidation. The only difference in the case of the Mn dimer is that the symmetry reduction from

(30) Kirchner, R. M.; Marks, T. J.; Kristoff, J. S.; Ibers, J. A. *J. Am. Chem. Soc.* **1973**, *95*, 6602–6613.

(31) The $2b_g$ orbital of **3** interacts nearly entirely with the CO 2π orbitals, yet it is stabilized to a similar extent as the orbitals that interact with NO 2π and much more so than the other orbitals with substantial CO 2π character. This is due to the high energy of the $2b_g$ orbital in the σ-only framework, placing it close in energy to the CO 2π set.

C_{2h} to C_1, due to asymmetric π-acid ligation, causes the HOMO of **3** to be somewhat localized on the Mn atom bound to the terminal CO ligand (ca. 66% to 12% polarization as shown.

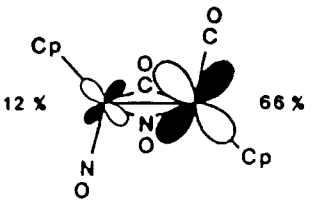

HOMO - 3

Therefore oxidation would result in the preferential removal of electron density from the Mn atom bound to the t-CO ligand and thus possibly result in the formation of a formal mixed-valence cation. Also, the metal–metal bond strengthening predicted during the oxidation of **1** may be diminished for $\mathbf{3}^+$, thereby inducing decomposition of the bimetallic radical cation. Possible products of such decomposition may be the stable monomeric cation $CpMn(CO)_2(NO)^+$[32] and the fragment [CpMn(NO)] which could oligomerize to form clusters such as the known $Cp_6Mn_6(NO)_8$.[8] The LUMO of **3** is also similar to that of the Fe dimer which undergoes irreversible cleavage. Once again, however, symmetry-reduction-induced orbital polarization causes the orbital to be more concentrated on the Mn atom bound to the t-CO ligand, although not to the extent as in the HOMO.

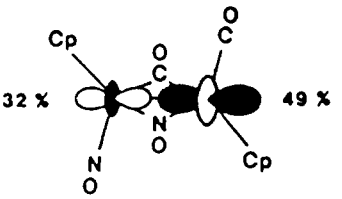

LUMO - 3

Hence, we would still predict dimer cleavage upon reduction and in all likelihood symmetrical cleavage (since the LUMO localization is not that significant) to yield the two two-legged piano-stool anions $CpMn(CO)(NO)^-$. This anion has never been isolated experimentally, however, even though several synthetic routes to this elusive anion have been attempted.[33] This is consistent with the results of Fenske–Hall calculations on $CpMn(CO)(NO)^-$, which have demonstrated that it would be thermodynamically unstable.[34] Thus the reduction of **3**, while predicted to parallel that of **1**, is expected to lead to unstable initial products and further decomposition.

Appendix

Molecular orbital calculations were performed on an IBM 3081-D computer system using the Fenske–Hall approximate MO method.[35] The atomic positions for $[CpFe(CO)]_2(\mu\text{-}CO)_2$,[16] $[CpCr(NO)]_2(\mu\text{-}NO)_2$,[36] and $[Cp_2Mn_2(CO)(NO)](\mu\text{-}CO)(\mu\text{-}NO)$[31] were taken from the crystal structures of the trans isomers in each case and idealized to C_{2h}, C_{2h}, and C_1 symmetry, respectively. Local D_{5h} symmetry has invoked upon the cyclopentadienyl rings, and a C–H distance of 1.08 Å was used for each dimer. The structures of the three σ-only model complexes $[CpCr(H)]_2(\mu\text{-}H)_2$, $[CpMn(H)]_2(\mu\text{-}H)_2$, and $[CpFe(H)]_2(\mu\text{-}H)_2$ were calculated by using the interatomic angles found in each of the parent π-acid dimers and assuming the following metal–hydride bond lengths: terminal hydride, Cr–H = 1.65 Å, Mn–H = 1.60 Å, Fe–H = 1.55 Å; bridging hydride, Cr–H = 1.75 Å, Mn–H = 1.70 Å, Fe–H = 1.65 Å.

All atomic wavefunctions were generated by using the method of Bursten, Jensen, and Fenske.[37] Contracted double-ζ representations were used for the Cr, Mn, and Fe 3d AO's and for the C, N, and O 2p AO's. An exponent of 1.16 was used for the hydrogen 1s AO.[38] The basis functions for Cr, Mn, and Fe were derived for the +1 oxidation state (s^0d^n) with the 4s exponents fixed at 2.0 and the 4p exponents fixed at 1.6, 1.8, and 2.0, respectively. The CO and NO 3σ orbitals, as well as the first three occupied C_5H_5 orbitals, were filled with 2.0 electrons and deleted from the basis transformation set in all calculations.[38] The CO and NO 6σ orbitals, as well as all virtual orbitals of C_5H_5 above the e_2'' level (D_{5h}), were filled with 0.0 electron and deleted from the basis transformation set in all calculations.[39]

The calculations were performed by using a fragment approach. In the case of the series $[CpM(EO)]_2(\mu\text{-}EO)]_2(\mu\text{-}EO)_2$, the EO ligands were converged as independent fragments, the resulting *molecular orbitals* of which were then allowed to interact with the Cp–M–M–Cp framework. The ligand CO was converged as a neutral molecule, whereas the NO ligands were converged as NO^+ for terminal coordination and NO^- for bridging coordination. The cyclopentadienyl ligands were all converged as Cp^-. All calculations were converged with a self-consistent field iterative technique by using a convergence criteria of 0.0010 as the largest deviation of atomic orbital populations between successive cycles.

Acknowledgment. We gratefully acknowledge Professor P. Legzdins for helpful discussions and results prior to publication. R.H.C. is grateful to The Ohio State University Graduate School for a Presidential Fellowship.

Registry No. **1**, 32757-46-3; **2**, 50277-98-0; **3**, 38999-59-6; $[CpFe(H)]_2(\mu\text{-}H)_2$, 114185-96-5; $[CpCr(H)]_2(\mu\text{-}H)_2$, 114185-97-6; $[CpMn(H)]_2(\mu\text{-}H)_2$, 114185-98-7.

(32) King, R. B.; Bisnette, M. B. *J. Am. Chem. Soc.* **1963**, *85*, 2527.
(33) (a) Kolthammer, B. W. S. Ph.D. Dissertation, University of British Columbia, 1979. (b) Legzdins, P.; Wassink, B., unpublished results. (c) The preparation of the third-row analogue $CpRe(CO)(NO)^-$ has also been attempted without success: Sweet, J. R.; Graham, W. A. G. *Organometallics* **1982**, *1*, 982–986.
(34) Gatter, M. G. Ph.D. Dissertation, The Ohio State University, 1985.
(35) Hall, M. B.; Fenske, R. F. *Inorg. Chem.* **1972**, *11*, 768–775.
(36) Calderon, J. L.; Fontana, S.; Frauendorfer, E.; Day, V. W. *J. Organomet. Chem.* **1974**, *64*, C10–C12.
(37) Bursten, B. E.; Jensen, J. R.; Fenske, R. F. *J. Chem. Phys.* **1978**, *68*, 3320–3321.
(38) Hehre, W. J.; Stewart, R. F.; Pople, J. A. *J. Chem. Phys.* **1969**, *51*, 2657–2664.
(39) Lichtenberger, D. L.; Fenske, R. F. *J. Chem. Phys.* **1976**, *64*, 4247–4264.